



Observation of $B^0 \rightarrow p\bar{\Lambda}\pi^-$

K. Abe,⁵ K. Abe,³⁶ T. Abe,³⁷ H. Aihara,³⁸ M. Akatsu,¹⁸ Y. Asano,⁴³ T. Aso,⁴² T. Aushev,⁸
A. M. Bakich,³³ Y. Ban,²⁸ E. Banas,²² A. Bay,¹⁴ P. K. Behera,⁴⁴ I. Bizjak,⁹ A. Bondar,¹
A. Bozek,²² M. Bračko,^{16,9} T. E. Browder,⁴ B. C. K. Casey,⁴ M.-C. Chang,²¹
P. Chang,²¹ Y. Chao,²¹ K.-F. Chen,²¹ B. G. Cheon,³² R. Chistov,⁸ Y. Choi,³²
Y. K. Choi,³² A. Drutskoy,⁸ S. Eidelman,¹ V. Eiges,⁸ C. Fukunaga,⁴⁰ N. Gabyshev,⁵
A. Garmash,^{1,5} T. Gershon,⁵ B. Golob,^{15,9} R. Guo,¹⁹ C. Hagner,⁴⁵ T. Hara,²⁶ M. Hazumi,⁵
T. Hojo,²⁶ T. Hokuue,¹⁸ Y. Hoshi,³⁶ W.-S. Hou,²¹ Y. B. Hsiung,^{21,*} H.-C. Huang,²¹
T. Igaki,¹⁸ Y. Igarashi,⁵ T. Iijima,¹⁸ K. Inami,¹⁸ A. Ishikawa,¹⁸ R. Itoh,⁵ H. Iwasaki,⁵
Y. Iwasaki,⁵ H. K. Jang,³¹ J. H. Kang,⁴⁶ J. S. Kang,¹¹ N. Katayama,⁵ H. Kawai,³⁸
T. Kawasaki,²⁴ H. Kichimi,⁵ D. W. Kim,³² H. J. Kim,⁴⁶ J. H. Kim,³² K. Kinoshita,³
S. Kobayashi,²⁹ P. Krokovny,¹ A. Kuzmin,¹ Y.-J. Kwon,⁴⁶ S. H. Lee,³¹ Y.-J. Lee,²¹
J. Li,³⁰ S.-W. Lin,²¹ D. Liventsev,⁸ J. MacNaughton,⁷ G. Majumder,³⁴ F. Mandl,⁷
T. Matsuishi,¹⁸ S. Matsumoto,² T. Matsumoto,⁴⁰ W. Mitaroff,⁷ H. Miyata,²⁴
G. R. Moloney,¹⁷ T. Mori,² T. Nagamine,³⁷ Y. Nagasaka,⁶ E. Nakano,²⁵ M. Nakao,⁵
H. Nakazawa,⁵ J. W. Nam,³² Z. Natkaniec,²² S. Nishida,¹² O. Nitoh,⁴¹ S. Ogawa,³⁵
T. Ohshima,¹⁸ T. Okabe,¹⁸ S. Okuno,¹⁰ S. L. Olsen,⁴ W. Ostrowicz,²² H. Ozaki,⁵
P. Pakhlov,⁸ H. Park,¹³ K. S. Park,³² M. Peters,⁴ L. E. Pilonen,⁴⁵ M. Rozanska,²²
K. Rybicki,²² H. Sagawa,⁵ S. Saitoh,⁵ Y. Sakai,⁵ M. Satapathy,⁴⁴ A. Satpathy,^{5,3}
O. Schneider,¹⁴ S. Schrenk,³ J. Schümann,²¹ A. J. Schwartz,³ S. Semenov,⁸ M. E. Seviar,¹⁷
H. Shibuya,³⁵ B. Shwartz,¹ V. Sidorov,¹ J. B. Singh,²⁷ S. Stanič,^{5,†} M. Starič,⁹ A. Sugi,¹⁸
T. Sumiyoshi,⁴⁰ S. Y. Suzuki,⁵ T. Takahashi,²⁵ F. Takasaki,⁵ K. Tamai,⁵ M. Tanaka,⁵
G. N. Taylor,¹⁷ Y. Teramoto,²⁵ S. Tokuda,¹⁸ T. Tsuboyama,⁵ T. Tsukamoto,⁵
S. Uehara,⁵ K. Ueno,²¹ S. Uno,⁵ G. Varner,⁴ K. E. Varvell,³³ C. C. Wang,²¹
C. H. Wang,²⁰ M.-Z. Wang,²¹ Y. Watanabe,³⁹ E. Won,¹¹ B. D. Yabsley,⁴⁵ Y. Yamada,⁵
Y. Yamashita,²³ M. Yamauchi,⁵ H. Yanai,²⁴ P. Yeh,²¹ Z. P. Zhang,³⁰ and D. Žontar^{15,9}

(The Belle Collaboration)

¹*Budker Institute of Nuclear Physics, Novosibirsk*

²*Chuo University, Tokyo*

³*University of Cincinnati, Cincinnati, Ohio 45221*

⁴*University of Hawaii, Honolulu, Hawaii 96822*

⁵*High Energy Accelerator Research Organization (KEK), Tsukuba*

- ⁶*Hiroshima Institute of Technology, Hiroshima*
⁷*Institute of High Energy Physics, Vienna*
⁸*Institute for Theoretical and Experimental Physics, Moscow*
⁹*J. Stefan Institute, Ljubljana*
¹⁰*Kanagawa University, Yokohama*
¹¹*Korea University, Seoul*
¹²*Kyoto University, Kyoto*
¹³*Kyungpook National University, Taegu*
¹⁴*Institut de Physique des Hautes Énergies, Université de Lausanne, Lausanne*
¹⁵*University of Ljubljana, Ljubljana*
¹⁶*University of Maribor, Maribor*
¹⁷*University of Melbourne, Victoria*
¹⁸*Nagoya University, Nagoya*
¹⁹*National Kaohsiung Normal University, Kaohsiung*
²⁰*National Lien-Ho Institute of Technology, Miao Li*
²¹*National Taiwan University, Taipei*
²²*H. Niewodniczanski Institute of Nuclear Physics, Krakow*
²³*Nihon Dental College, Niigata*
²⁴*Niigata University, Niigata*
²⁵*Osaka City University, Osaka*
²⁶*Osaka University, Osaka*
²⁷*Panjab University, Chandigarh*
²⁸*Peking University, Beijing*
²⁹*Saga University, Saga*
³⁰*University of Science and Technology of China, Hefei*
³¹*Seoul National University, Seoul*
³²*Sungkyunkwan University, Suwon*
³³*University of Sydney, Sydney NSW*
³⁴*Tata Institute of Fundamental Research, Bombay*
³⁵*Toho University, Funabashi*
³⁶*Tohoku Gakuin University, Tagajo*
³⁷*Tohoku University, Sendai*
³⁸*University of Tokyo, Tokyo*
³⁹*Tokyo Institute of Technology, Tokyo*
⁴⁰*Tokyo Metropolitan University, Tokyo*
⁴¹*Tokyo University of Agriculture and Technology, Tokyo*
⁴²*Toyama National College of Maritime Technology, Toyama*
⁴³*University of Tsukuba, Tsukuba*
⁴⁴*Utkal University, Bhubaneswer*
⁴⁵*Virginia Polytechnic Institute and State University, Blacksburg, Virginia 24061*
⁴⁶*Yonsei University, Seoul*

Abstract

We report the first observation of the charmless hyperonic B decay, $B^0 \rightarrow p\bar{\Lambda}\pi^-$, using a 78 fb^{-1} data sample recorded on the $\Upsilon(4S)$ resonance with the Belle detector at KEKB. The measured branching fraction is $\mathcal{B}(B^0 \rightarrow p\bar{\Lambda}\pi^-) = (3.97_{-0.80}^{+1.00} \pm 0.56) \times 10^{-6}$. Searches for $B^0 \rightarrow p\bar{\Lambda}K^-$ and $p\bar{\Sigma}^0\pi^-$ yield no significant signals and we set 90% confidence level upper limits of $\mathcal{B}(B^0 \rightarrow p\bar{\Lambda}K^-) < 8.2 \times 10^{-7}$ and $\mathcal{B}(B^0 \rightarrow p\bar{\Sigma}^0\pi^-) < 3.8 \times 10^{-6}$.

PACS numbers: PACS numbers: 13.20.H

The Belle collaboration recently reported the observation of $B^+ \rightarrow p\bar{p}K^+$ [1], which is the first known example of B meson decay to charmless final states containing baryons. The three-body decay rate is larger than the rate for two-body decays (such as $B \rightarrow p\bar{p}$ [2]), and the observed $M_{p\bar{p}}$ spectrum peaks near threshold, in agreement with theoretical suggestions [3, 4]. In this paper we report the first observation of the related three-body decay $B^0 \rightarrow p\bar{\Lambda}\pi^-$, and a search for $B^0 \rightarrow p\bar{\Lambda}K^-$ and $p\bar{\Sigma}^0\pi^-$ modes. The rate for $B^0 \rightarrow p\bar{\Lambda}\pi^-$ is comparable to $B^+ \rightarrow p\bar{p}K^+$, and the observed $M_{p\bar{\Lambda}}$ spectrum again peaks toward threshold.

In the Standard Model, these decays proceed via $b \rightarrow u$ tree and $b \rightarrow s(d)$ penguin diagrams. They may be used to search for direct CP violation and test our theoretical understanding of rare decay processes involving baryons [3, 4, 5, 6, 7]. Modes involving hyperons, in particular, can probe the s quark chirality in B decay [8]; with sufficient statistics, they could provide a tool for probing T violation [3] via the self-analyzed Λ polarization information.

We use a 78 fb^{-1} data sample, consisting of 85.0 ± 0.5 million $B\bar{B}$ pairs, collected by the Belle detector at the KEKB asymmetric energy e^+e^- (3.5 on 8 GeV) collider. The Belle detector is a large-solid-angle magnetic spectrometer that consists of a three-layer silicon vertex detector (SVD), a 50-layer central drift chamber (CDC), an array of aerogel threshold Čerenkov counters (ACC), a barrel-like arrangement of time-of-flight scintillation counters (TOF), and an electromagnetic calorimeter comprised of CsI(Tl) crystals located inside a super-conducting solenoid coil that provides a 1.5 T magnetic field. An iron flux-return located outside of the coil is instrumented to detect K_L^0 mesons and to identify muons. The detector is described in detail elsewhere [9].

Since the e^+e^- center-of-mass energy is set to match the $\Upsilon(4S)$ resonance, which decays into a $B\bar{B}$ pair, one can use the following two kinematic variables to identify the reconstructed B meson candidates [10]: the beam-energy constrained mass, $M_{bc} = \sqrt{E_{\text{beam}}^2 - p_B^2}$, and the energy difference, $\Delta E = E_B - E_{\text{beam}}$, where E_{beam} is the beam energy, and p_B and E_B are the momentum and energy of the reconstructed B meson in the $\Upsilon(4S)$ rest frame. The candidate region is defined as $5.2 \text{ GeV}/c^2 < M_{bc} < 5.29 \text{ GeV}/c^2$ and $|\Delta E| < 0.2 \text{ GeV}$ in this analysis.

The event selection criteria are based on the information obtained from the tracking system (SVD+CDC) and the hadron identification system (CDC+ACC+TOF), and are optimized using Monte Carlo (MC) simulated event samples.

All primary charged tracks are required to satisfy track quality criteria based on the track impact parameters relative to the interaction point (IP). The deviations from the IP position are required to be within $\pm 0.3 \text{ cm}$ in the transverse (x - y) plane, and within $\pm 3 \text{ cm}$ in the z direction, where the z axis is defined by the positron beam line. Primary proton candidates are selected based on $p/K/\pi$ likelihood functions obtained from the hadron identification system. We require $L_p/(L_p + L_K) > 0.3$ and $L_p/(L_p + L_\pi) > 0.6$, where $L_{p/K/\pi}$ stands for the proton/kaon/pion likelihood. For kaons (pions), we require the kaon (pion) K - π likelihood ratio to be greater than 0.6. Λ candidates are reconstructed via the $p\pi^-$ decay channel using the method described in Ref. [2]. Σ^0 candidates are reconstructed via the $\Lambda\gamma$ decay channel, where we use a $35 \text{ MeV}/c^2$ mass window around the nominal mass [11] and require the γ energy to be greater than 100 MeV.

The dominant background for the rare decay modes reported here is from the continuum $e^+e^- \rightarrow q\bar{q}$ process. The background from B decays is much smaller. This is confirmed with an off-resonance data set (8.8 fb^{-1}) accumulated at an energy that is 60 MeV below the $\Upsilon(4S)$, and an MC sample of 120 million continuum events. In the $\Upsilon(4S)$ rest frame,

continuum events are jet-like while $B\bar{B}$ events are spherical. We follow the scheme defined in Ref. [12] and combine seven shape variables to form a Fisher discriminant [13] that is used to optimize continuum background suppression. The variables chosen have almost no correlation with M_{bc} and ΔE . Probability density functions (PDF's) for the Fisher discriminant and the cosine of the angle between the B flight direction and the e^- beam direction in the $\Upsilon(4S)$ rest frame are combined to form the signal (background) likelihood $\mathcal{L}_{S(BG)}$. We require the likelihood ratio $\mathcal{LR} = \mathcal{L}_S / (\mathcal{L}_S + \mathcal{L}_{BG})$ to be greater than 0.8, which suppresses about 94% of the background while retaining 66% of the signal. The signal and background PDF's are obtained from MC simulation studies.

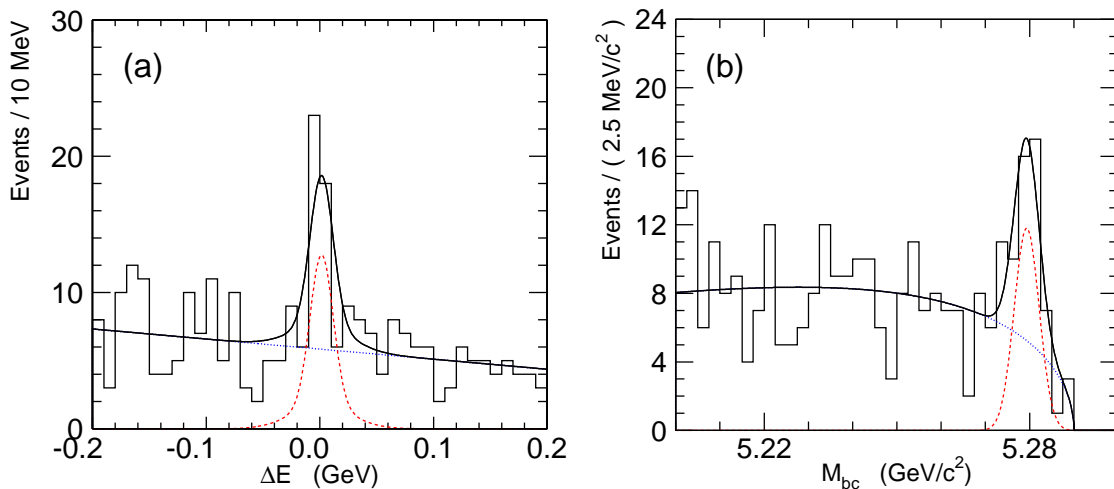


FIG. 1: The (a) ΔE and (b) M_{bc} distributions for $B^0 \rightarrow p\bar{\Lambda}\pi^-$ candidates. The solid, dotted and dashed lines represent the combined fit result, fitted background and fitted signal, respectively.

Figure 1(a) shows the ΔE distribution for selected $p\bar{\Lambda}\pi^-$ candidates that have $M_{bc} > 5.27 \text{ GeV}/c^2$; Fig. 1(b) shows the M_{bc} distribution for events with $|\Delta E| < 0.03 \text{ GeV}$. With the current statistics, no intermediate resonances are evident in the Dalitz plot for this channel. We use a binned likelihood fit to estimate the signal yield. A Gaussian is used to parameterize the signal in M_{bc} while a double Gaussian is used for ΔE . The Gaussian parameters are determined from MC simulation. Background shapes are studied using side-band events ($0.1 \text{ GeV} < |\Delta E| < 0.2 \text{ GeV}$ for the M_{bc} study and $5.20 \text{ GeV}/c^2 < M_{bc} < 5.26 \text{ GeV}/c^2$ for ΔE) and are checked with the continuum MC sample. We use the ARGUS function [14] to model the M_{bc} background and a linear function for the ΔE background. The fit results are shown as curves in Fig. 1. The fit to the ΔE distribution yields $39.2^{+9.1}_{-8.4}$ candidates with a significance of 5.8 standard deviations. The fit to the M_{bc} distribution yields $33.7^{+8.1}_{-7.4}$ candidates with a significance of 5.7 standard deviations. The smaller yield in the M_{bc} fit is consistent with the ΔE fit result after taking into account the efficiency of the $|\Delta E| < 0.03 \text{ GeV}$ selection. The signal yields and the branching fractions are determined from fits to the ΔE distribution rather than to M_{bc} in order to minimize possible bias from $B\bar{B}$ background, which tends to peak in M_{bc} but not in ΔE .

Since the decay is not uniform in phase space, we fit the ΔE signal yield in bins of $M_{p\bar{\Lambda}}$,

TABLE I: The event yield, efficiency, and branching fraction (\mathcal{B}) for each $M_{p\bar{\Lambda}}$ bin.

$M_{p\bar{\Lambda}}$ (GeV/ c^2)	signal yield	efficiency(%)	\mathcal{B} (10^{-6})
< 2.2	$11.4^{+4.0}_{-3.3}$	12.5	$1.08^{+0.37}_{-0.31}$
$2.2 - 2.4$	$11.2^{+4.4}_{-3.7}$	11.7	$1.12^{+0.44}_{-0.37}$
$2.4 - 2.6$	$2.4^{+2.7}_{-2.0}$	11.1	$0.25^{+0.29}_{-0.21}$
$2.6 - 2.8$	$2.4^{+2.6}_{-1.8}$	9.9	$0.28^{+0.31}_{-0.22}$
$2.8 - 3.4$	$2.4^{+2.9}_{-2.2}$	11.4	$0.24^{+0.30}_{-0.23}$
$3.4 - 4.0$	$5.0^{+3.6}_{-2.8}$	11.7	$0.51^{+0.36}_{-0.29}$
$4.0 - 4.6$	$-3.3^{+2.3}_{-1.8}$	12.5	$-0.31^{+0.21}_{-0.17}$
> 4.6	$7.0^{+4.2}_{-3.5}$	10.4	$0.79^{+0.48}_{-0.39}$

and correct for the MC-determined detection efficiency for each bin. This reduces the model dependence of the branching fraction determination. The signal yield as a function of $p\bar{\Lambda}$ mass is shown in Fig. 2. The distribution from a three-body phase space MC, normalized to the area of the signal, is superimposed. The observed mass distribution peaks at low $p\bar{\Lambda}$ mass, similar to that observed for $B^+ \rightarrow p\bar{p}K^+$ decays [1]. The results of the fits, along with the efficiencies and partial branching fractions for each $M_{p\bar{\Lambda}}$ bin, are given in Table I. We sum the partial branching fractions in Table I to obtain

$$\mathcal{B}(B^0 \rightarrow p\bar{\Lambda}\pi^-) = (3.97^{+1.00}_{-0.80} \text{ (stat)} \pm 0.56 \text{ (syst)}) \times 10^{-6},$$

where the systematic uncertainty is described below.

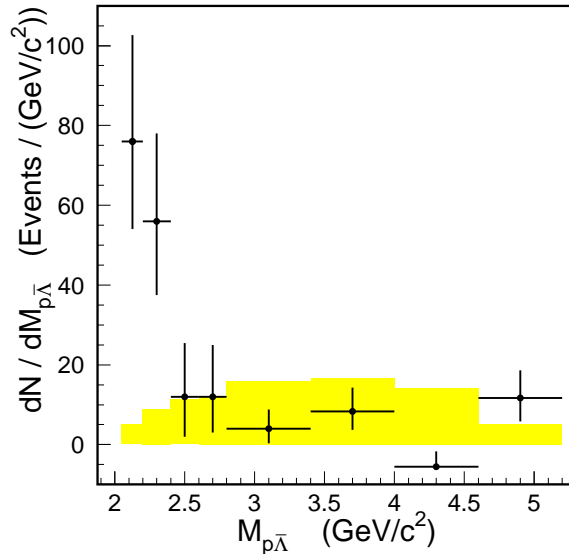


FIG. 2: The fitted yield divided by the bin size for $B^0 \rightarrow p\bar{\Lambda}\pi^-$ as a function of $M_{p\bar{\Lambda}}$. The shaded distribution is from a phase-space MC simulation with area normalized to signal yield.

The systematic uncertainty in particle selection is studied mainly using high statistics control samples. Proton identification is studied with a $\Lambda \rightarrow p\pi^-$ sample. Kaon/pion identification is studied with a $D^{*+} \rightarrow D^0\pi^+$, $D^0 \rightarrow K^-\pi^+$ sample. Tracking efficiency is studied with $\eta \rightarrow \gamma\gamma$ and $\eta \rightarrow \pi^+\pi^-\pi^0$ samples. Based on these studies, we assign a 2% error for each track, 3% for each proton identification requirement, and 2% for each kaon/pion identification requirement.

We study the \mathcal{LR} continuum suppression by varying the \mathcal{LR} cut value from 0 to 0.9 to check the systematic trend. The systematic error is found to be 4%. The additional uncertainty of off-IP tracks for Λ reconstruction is estimated to be 6%, which is determined from the difference of the proper decay time distributions for data and MC simulation.

The systematic uncertainty in the fit yield is studied by varying the parameters of the signal and background PDF's. We assign an error of 3% for this. The MC statistical uncertainty and modeling with eight $M_{p\bar{\Lambda}}$ bins contributes a 4% error in the branching fraction determination. The error on the number of total $B\bar{B}$ pairs is determined to be 1%. The error of the branching fraction for $\Lambda \rightarrow p\pi^-$ is 0.8% [11].

We sum the correlated errors linearly (i.e. 8% error for tracking and 8% for particle identification) and then combine them in quadrature with the uncorrelated errors to determine a total systematic error of 14%.

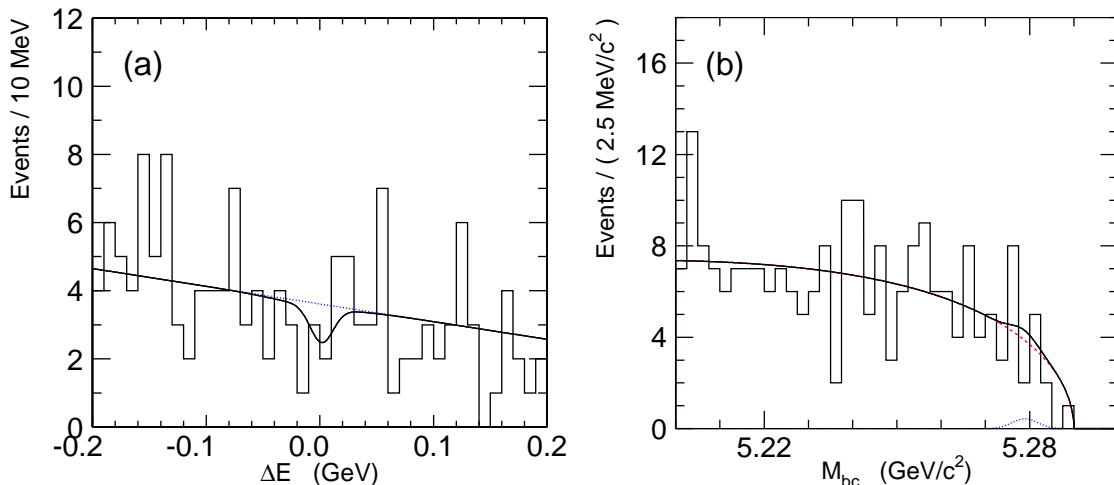


FIG. 3: The (a) ΔE and (b) M_{bc} distributions for $B^0 \rightarrow p\bar{\Lambda}K^-$ candidates. The solid line represents the fit results.

We also search for the decay modes $B^0 \rightarrow p\bar{\Lambda}K^-$ and $B^0 \rightarrow p\bar{\Sigma}^0\pi^-$. The M_{bc} and ΔE distributions with fit projections are shown in Figs. 3 and 4. With the signal region extended to $|\Delta E| < 0.04$ GeV and $M_{bc} > 5.27$ GeV/c^2 , no significant signal is found. We use the fit results to estimate the expected background, and compare this with the observed number of events in the signal region in order to set the upper limit on the yield at the 90% confidence level [15, 16, 17]. This procedure takes systematic uncertainties into account. The estimated backgrounds are 28.9 ± 2.6 and 50.5 ± 4.0 , the numbers of observed events are 26 and 56, the systematic uncertainties are 14% and 28%, and the upper limit yields are 8.3 and 22.4 for $p\bar{\Lambda}K^-$ and $p\bar{\Sigma}^0\pi^-$, respectively. We estimate the efficiencies from a phase

space MC sample. The 90% confidence level upper limits for the branching fractions are $\mathcal{B}(B^0 \rightarrow p\bar{\Lambda}K^-) < 8.2 \times 10^{-7}$ and $\mathcal{B}(B^0 \rightarrow p\bar{\Sigma}^0\pi^-) < 3.8 \times 10^{-6}$.

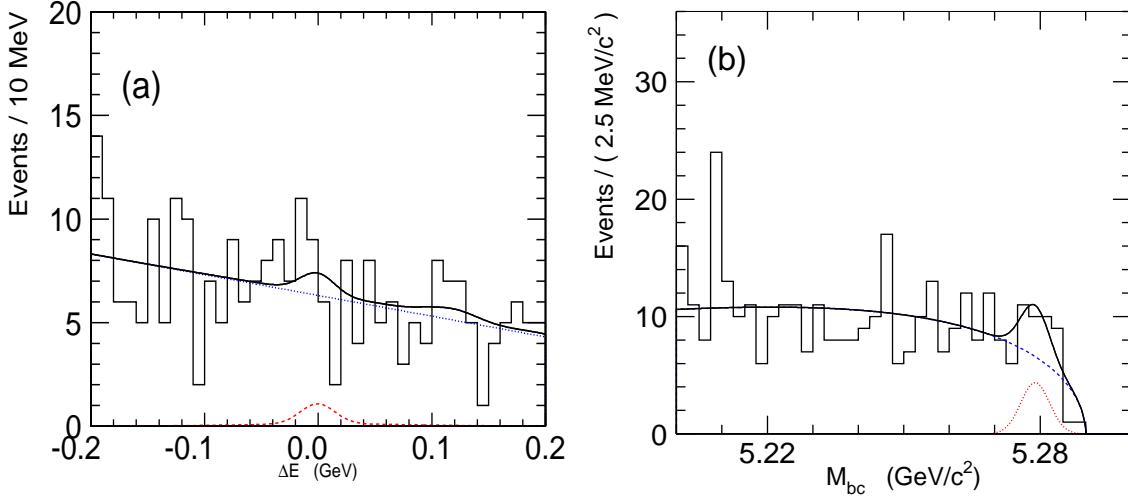


FIG. 4: The (a) ΔE and (b) M_{bc} distributions for $B^0 \rightarrow p\bar{\Sigma}^0\pi^-$ candidates. Note that events from $B^0 \rightarrow p\bar{\Lambda}\pi^-$ decay can feed into the high ΔE region (~ 0.1 GeV). The corresponding distribution is obtained from the $p\bar{\Lambda}\pi^-$ MC and included in the fit.

Following our observation of the $B^+ \rightarrow p\bar{p}K^+$ mode, some authors [6, 7] predicted a much smaller branching fraction ($< 10^{-6}$) for the $B^0 \rightarrow p\bar{\Lambda}\pi^-$ mode, but a relatively sizable $B^0 \rightarrow p\bar{\Sigma}^0\pi^-$. Although the predicted rates are not borne out by our present findings, the threshold peaking behavior shown in Fig. 2 was anticipated [3, 4, 7].

In summary, we have performed a search for the rare baryonic decays $B^0 \rightarrow p\bar{\Lambda}\pi^-$, $p\bar{\Lambda}K^-$, and $p\bar{\Sigma}^0\pi^-$ with 85.0 ± 0.5 million $B\bar{B}$ events. A clear signal is seen in the $p\bar{\Lambda}\pi^-$ mode, and we measure a branching fraction of $\mathcal{B}(B^0 \rightarrow p\bar{\Lambda}\pi^-) = (3.97_{-0.80}^{+1.00} \pm 0.56) \times 10^{-6}$. The other two modes are not seen, and we set 90% confidence level upper limits of $\mathcal{B}(B^0 \rightarrow p\bar{\Lambda}K^-) < 8.2 \times 10^{-7}$ and $\mathcal{B}(B^0 \rightarrow p\bar{\Sigma}^0\pi^-) < 3.8 \times 10^{-6}$.

We wish to thank the KEKB accelerator group for the excellent operation of the KEKB accelerator. We acknowledge support from the Ministry of Education, Culture, Sports, Science, and Technology of Japan and the Japan Society for the Promotion of Science; the Australian Research Council and the Australian Department of Industry, Science and Resources; the National Science Foundation of China under contract No. 10175071; the Department of Science and Technology of India; the BK21 program of the Ministry of Education of Korea and the CHEP SRC program of the Korea Science and Engineering Foundation; the Polish State Committee for Scientific Research under contract No. 2P03B 17017; the Ministry of Science and Technology of the Russian Federation; the Ministry of Education, Science and Sport of the Republic of Slovenia; the National Science Council and the Ministry of Education of Taiwan; and the U.S. Department of Energy.

* on leave from Fermi National Accelerator Laboratory, Batavia, Illinois 60510

† on leave from Nova Gorica Polytechnic, Nova Gorica

- [1] K. Abe *et al.* (Belle Collaboration), Phys. Rev. Lett. **88**, 181803 (2002).
- [2] K. Abe *et al.* (Belle Collaboration), Phys. Rev. D **65**, 091103 (2002).
- [3] W.S. Hou and A. Soni, Phys. Rev. Lett. **86**, 4247 (2001).
- [4] C.K. Chua, W.S. Hou and S.Y. Tsai, Phys. Lett. **B528**, 233 (2002).
- [5] F. Piccinini and A.D. Polosa, Phys. Rev. D **65**, 097508 (2002); H.Y. Cheng and K.C. Yang, Phys. Lett. **B533**, 271 (2002).
- [6] H.Y. Cheng and K.C. Yang, Phys. Rev. D **66**, 014020 (2002).
- [7] C.K. Chua, W.S. Hou and S.Y. Tsai, Phys. Rev. D **66**, 054004 (2002).
- [8] M. Suzuki, hep-ph/0208060.
- [9] A. Abashian *et al.* (Belle Collaboration), Nucl. Instr. and Meth. A **479**, 117 (2002).
- [10] Throughout this report, inclusion of charge conjugate mode is always implied unless otherwise stated.
- [11] K. Hagiwara *et al.* (Particle Data Group), Phys. Rev. D **66**, 010001 (2002).
- [12] K. Abe *et al.* (Belle Collaboration), Phys. Lett. **B517**, 309 (2001).
- [13] R.A. Fisher, Annals of Eugenics **7**, 179 (1936).
- [14] H. Albrecht *et al.*, Phys. Lett. **B241**, 278 (1990); *ibid.* **B254**, 288 (1991).
- [15] R.D. Cousins and V.L. Highland, Nucl. Instr. and Meth. A **320**, 331 (1993).
- [16] G.J. Feldman and R.D. Cousins, Phys. Rev. D **57**, 3873 (1998).
- [17] J. Conrad *et al.*, hep-ex/0202013.